
Technical Note

QUANTITATIVE ANALYSIS OF ROCK SAMPLES BY AN X-RAY FLUORESCENCE SPECTROMETER (II)

GOTO, ATSUSHI

Himeji Institute of Technology, Shosha, Himeji, Hyogo 671-22, Japan

TATSUMI, YOSHIYUKI

Kyoto University, Faculty of Science, Kitashirakawaiwake, Sakyo-ku, Kyoto 606-01, Japan

1. Introduction

One of the advantages of X-ray fluorescence XRF analysis is its ability to perform accurate quantitative analysis over a wide range of elements with relative ease. In addition, its high sensitivity makes it ideal for trace elemental analysis. The establishment of analytical conditions for XRF is straightforward, including the determination of spectral line overlap correction factors. As with most analytical techniques, matrix effects (inter-element effects) need to be corrected for when performing quantitative analysis. XRF analysis also requires careful selection of analytical standards to achieve optimum quantitative results.

In the first half of this article, quantitative analysis of briquette samples will be summarized. This work was performed with an X-ray spectrometer in collaboration with the Analytical Laboratory at Rigaku Industrial Corporation. Analytical methods for trace analysis of elements such as Nb, Zr, Y, Sr, Rb, Pb, Th, Ni, Ba, Cl, Na and K will be discussed. In the second half, analytical methods for the quantitative analysis of major elements in briquette samples will be summarized. The method discussed is not applicable for every element because of general difficulties encountered with SiO_2 and Al_2O_3 contents. However, these results will also be summarized. SiO_2 is the major constituent of most rocks; and, Al_2O_3 presents analytical difficulties even by wet techniques. Please refer to "Quantitative analysis of rock samples by an X-ray fluorescence spectrometer (1) by Goto and Tatsumi (1994)" for information on the preparation of briquette samples.

Trace Elemental Analysis

2. Determination of Measurement Conditions

Qualitative analysis of JB-1a, JG-1a and JGb-1 briquettes was performed utilizing the conditions shown in Table 1. These conditions allow one to determine the interaction between Ba and Ti. Preliminary qualitative analysis enables one to determine precise peak and background positions, the presence of trace elements, the extent of changes in X-ray intensity as the chemical composition varies, and which elements require an overlap correction.

The observed X-ray intensity is the sum of characteristic and continuous X-rays. At the low angle area, where the slope of the background is steep, the observed peak position of trace elements does not match the true peak position. (See JGb-1 of Rb). Therefore, the peak position of an element, which has no spectral overlap, should be determined with a sample containing a sufficient amount of that element. Optimum background positions are selected by comparing results from qualitative analysis. (One should study the full scale results of the data to determine the best intensity variation.)

The peak position of an element influenced by spectral overlap is determined by utilizing a high purity sample or a known prepared mixture. The peak

Table 1 Conditions of JB-1a, JG-1a and JGb-1 step scans

Examination of the $\text{TiK}\alpha$ and $\text{BaL}\alpha$ relationship	
10 sec/1 step	0.02°/1 step
crystal: LiF	counter: SC slit: coarse
smoothing: 11	PHA: 100-300
scanning angle:	82-95°

Table 2 Measurement conditions employed for the Rigaku 3370 spectrometer

Voltage: 50 kV Current: 50 mA
 Anode: Rh (Rhodium) (X-ray tube: Rhodium tube)
 Beam path: vacuum

Elements (X-ray lines)	Peak	BG1 (low)	BG2 (high)	Diffraction crystal	Slit	Counter	Time (sec)	PHA
*TiK α	86.17	82.50	89.50	LiF1	coarse	SC	100	100-300
TiK α	86.17	82.50	89.50	LiF3	fine	F-PC	100	100-300
BaL α	87.18	84.68	88.68	LiF1	coarse	SC	100	100-300
*BaL α	87.18	82.50	89.50	LiF1	coarse	SC	100	100-300
BaL α	87.18	84.68	88.68	LiF3	fine	F-PC	100	100-300
BaL α	87.18	82.50	89.50	LiF3	fine	F-PC	100	100-300
*NiK α	48.68	48.10	49.20	LiF1	coarse	SC	100	100-300
PbL α	33.94	33.55	34.50	LiF1	coarse	SC	200	100-300
PbL α	33.94	33.55	34.50	LiF	fine	SC	200	100-300
PbL β	28.25	27.78	28.68	LiF11	coarse	SC	200	100-280
*PbL β	28.25	27.85	28.65	LiF1	fine	SC	200	100-280
*ThL α	27.46	27.10	27.78	LiF1	fine	SC	200	100-300
*RbK α	26.62	26.00	27.10	LiF1	fine	SC	200	100-300
*SrK α	25.15	24.62	25.90	LiF	fine	SC	100	100-300
*YK α	23.81	23.10	24.50	LiF1	fine	SC	100	100-300
*NbK α	21.40	21.00	21.80	LiF1	fine	SC	200	100-300
*ZrK α	22.56	21.80	23.10	LiF1	fine	SC	100	100-300
*NaK α	55.16	52.00	59.00	TAP	coarse	F-PC	100	150-250
*KK α	136.64	130.50	141.50	LiF3	coarse	F-PC	100	100-300
*ClK α	92.825	91.50	94.20	Ge	coarse	F-PC	100 (BG40)	150-300

* used in this experiment

positions of Nb, Zr, Y, Pb and Ba were determined using pure niobium and Nb₂O₅-SiO₂ mixture, pure zirconium and ZrO₂-SiO₂ mixture, Y₂O₃-SiO₂ mixture, Pb rich compound, and Ba rich compound and BaCO₃-SiO₂ mixture, respectively. The TiK α position used for the overlap correction of the BaLa line was determined with a TiO₂-SiO₂ mixture.

Peak positions must be confirmed because some differences are expected between the 20 table (measured at 20°C) and the peak positions measured at the actual sample chamber temperature (36.5°C); instrumental dependence can also influence the position.

An appropriate detector, analyzing crystal and soller slit need to be selected. The combination of a LiF crystal and a scintillation counter (SC) detector is typically used for the high energy region. At the low energy region, a gas flow type proportional counter detector should be employed, but there are more options for analyzing crystals. At the intermediate energy region, the detector also needs to be selected.

Basically, one should choose a combination that gives the best counting statistics. For this work, a coarse soller slit (3S) was used for elements without peak overlap while a fine soller slit (1S) was used for elements that have peaks in close proximity. In Pb analysis, the L β line was selected over L α because the AsL β overlaps the PbL α line. The affect of the secondary K α line on the L β line was eliminated by reducing the upper limit of the pulse height analyzer from 300 to 280. For Na analysis, the window of the pulse height analyzer was narrowed to 150-250 to eliminate the effect of high-order emission from thallium on a TAP crystal.

Table 2 shows the measurement conditions determined by preliminary experiments. Measurement conditions of some elements required further consideration.

3. Overlap Correction

The overlaps of the TiK α line to the BaL α line, the YK β line to the NbK α line, the SrK β line to the ZrK α line, and the RbK β line to the YK α line were corrected. Also, matrix effects were corrected for in this experiment by using background intensity measurements (See below). Therefore, not only the overlap of peaks but also the overlap to the background were corrected. Standards were prepared by mixing commercially available chemicals to determine the overlap correction coefficient, to maintain the dead time of the counter at a proper level, and to minimize the counting error simultaneously. Appendix 2.2 summarizes the preparation of the standards.

3.1 The Overlap Correction of the TiK α Line to the BaL α Line

For the analysis of Ba, both SC and F-PC detectors can be used with the LiF analyzing crystal. An F-PC has lower resolution, but a higher counting rate than a SC. Therefore, an F-PC gives better counting statistics on background X-ray intensity and improves the accuracy.

TiO₂ free sample and TiO₂-SiO₂ mixed sample were brisquitted and analyzed with the conditions shown in Table 3 to confirm the background shape and the absence of any impurity that could affect the overlap correction. (For example, the secondary line of Zn appeared with the TiO₂ (rutile) for chemistry grade chemicals obtained from Wako Chemicals, but the -5 μ m 99.9% TiO₂ (rutile) from Wako did not show the secondary line of Zn. Therefore, it was decided to use the latter.) First, the previously determined measurement positions (Table 2) were checked and then the X-ray intensity of the mixture was measured. These measurements should be done at six points for each F-PC and SC, and the overlap correction coefficient of the TiK α line to the BaL α line.

Table 3 An example of conditions of qualitative analysis used as the basis of the TiK α line overlap

SC counter
Diffraction crystal: LiF, soller slit: coarse (3S)
Step scan: 4 sec/setp, 0.02°/step, smoothing: 11 pts,
2 θ : 82-92°, PHA: 100-300
F-PC counter
Diffraction crystal: LiF, counter: F-PC, soller slit: fine (1S)
Step scan: 4 sec/setp, 0.02°/step, smoothing: 11 pts,
2 θ : 82-92°, PHA: 100-300

Note: Determination of the Background X-ray Intensity at a Peak Position

The background intensity at a peak position is determined by calculation. There are two methods. One is to estimate from the slope of the background and the other is to interpolate from the intensities at higher and lower angle sides of a peak. The former method is effective when one of the background intensities are indeterminable due to peak overlap. The background at the titanium and barium positions were checked and it was found that the slope was not constant. Therefore, it was decided to estimate the background by the linear interpolation of the background intensities at the higher and lower sides of a peak. The background intensity and the net peak intensity were calculated as shown below.

The equation to calculate the background intensity at a peak position:

$$IBG = \frac{(2\theta BG2 - 2\theta Peak) * IBG1 + (2\theta Peak - 2\theta BG1) * IBG2}{(2\theta BG2 - 2\theta BG1)}$$

The equations to calculate the net peak intensity:

$$INPeak = IPeak - IBG$$

Here, I: X-ray intensity; 2 θ : measurement position (angle)

BG1, BG2: background at higher energy side (low angle) and lower energy side (high angle) Peak: Peak; Npeak: Net peak; BG: background at a peak position

* * * *

Both the background and peak intensities of the TiK α line and the BaL α line from the SiO₂-TiO₂ mixture were measured. The net peak intensity of the TiK α line was calculated from the background and peak intensities. The influence on the peak and the background positions of the BaL α line was calculated as a ratio against the net X-ray intensity of the TiK α line. This ratio is the overlap correction coefficient for the peak and background.

Determination of the overlap correction coefficient with LiF-SC-coarse slit (3S) Measurements for 100 seconds were repeated three times. The results are shown in Table 4 and the overlap correction coefficients from that data are listed in Table 5.

A series of measurements at different TiO₂ concentrations shows that the overlap correction coefficient at the BaL α line peak position is independent from the TiO₂ concentration; therefore, the BaL α line to the net TiK α line intensity ratio is constant. The

Table 4 An example of the results corrected for the TiK α line overlap on the BaL α line

Sample: low TiO ₂ -SiO ₂	TiK α position			BaL α position		
	BG1	peak	BG2	BG1	peak	BG2
1 (kcps)	0.0786	11.726	0.0638	0.0781	0.0930	0.0660
2	0.0795	11.715	0.0628	0.0802	0.0908	0.0670
3	0.0791	11.731	0.0656	0.0786	0.0938	0.0664
average	0.0791	11.724	0.0641	0.0790	0.0925	0.0665
maximum	0.0795	11.731	0.0656	0.0802	0.0938	0.0670
minimum	0.0786	11.715	0.0628	0.0781	0.0908	0.0660
range	0.0009	0.016	0.0028	0.0021	0.0030	0.0010
standard deviation (1 σ)	0.00045	0.0082	0.00142	0.00110	0.00155	0.00050
fluctuation coefficient	0.57	0.07	2.21	1.39	1.68	0.76
average (C)	7910	1172400	6410	7900	9250	6650
counting error (1 σ)	88.9	1082.9	80.1	88.9	96.2	81.5
1 σ /C (%)	1.12	0.09	1.25	1.13	1.04	1.23
average	0.0791	11.724	0.0641	0.0790	0.0925	0.0665
IBG (cal.)		0.0712		0.0744	0.0691	0.0659
difference		11.653		0.0046	0.0234	0.0006
correction coefficient		1		0.000395	0.002008	0.000051

Sample: high TiO ₂ -SiO ₂	TiK α position			BaL α position		
	BG1	peak	BG2	BG1	peak	BG2
1 (kcps)	0.0875	32.952	0.0716	0.1004	0.1426	0.0823
2	0.0869	32.933	0.0724	0.1013	0.1451	0.0804
3	0.0884	32.938	0.0719	0.1014	0.145	0.0827
average	0.0876	32.941	0.0719	0.1010	0.144	0.0818
maximum	0.0884	32.952	0.0724	0.1014	0.1451	0.0827
minimum	0.0869	32.933	0.0716	0.1004	0.1426	0.0804
range	0.0015	0.019	0.0008	0.0010	0.0025	0.0023
standard deviation (1 σ)	0.00075	0.0098	0.0008	0.00055	0.00144	0.00123
fluctuation coefficient	0.86	0.03	0.56	0.55	1.00	1.50
average (C)	8760	3294100	7200	10100	14430	8180
counting error (1 σ)	93.6	1815.0	84.9	100.5	120.1	73.8
1 σ /C (%)	1.07	0.06	1.18	0.995	0.83	1.1
average	0.0876	32.941	0.0719	0.1010	0.1443	0.0818
IBG (cal.)		0.0794		0.0827	0.0772	0.0738
difference		32.862		0.0183	0.0671	0.0060
correction coefficient		1		0.000557	0.002042	0.000243

BaL α intensity of a rock sample is the residual of the subtraction of 0.0020 times the net TiK α line intensity from the X-ray intensity at $2\theta=87.18^\circ$. The back-

ground intensity calculated from the TiK α line background intensity was first used as the true BaL α line background intensity. However, it was found to be essentially meaningless, to result in larger errors, and to cause unnecessary complexity. Therefore, the background intensity of the BaL α line was measured at the same position as that of the TiK α line.

Determination of the overlap correction coefficient with LiF-F-PC-fine slit (IS) Measurements for 100 seconds were repeated three times. The results are shown in Table 6 and the overlap correction coefficients calculated from the data are listed in Table 7.

Table 5 Overlap correction coefficients of the TiK α line overlap on the BaL α line

	BG1	Peak	BG2
low-Ti correction coefficients	0.000395	0.002008	0.000051
high-Ti correction coefficients	0.000557	0.002042	0.000243
average		0.0020	

Table 6 An example of the results corrected for the TiK α line overlap on the BaL α line

Sample: low TiO ₂ -SiO ₂	TiK α position			BaL α position		
	BG1	peak	BG2	BG1	peak	BG2
1 (kcps)	0.2094	36.019	0.1565	0.2331	0.3385	0.1731
2	0.2086	35.997	0.1551	0.2342	0.3361	0.1741
3	0.2066	36.016	0.1558	0.2326	0.3387	0.1738
average	0.2082	36.011	0.1558	0.2333	0.3378	0.1737
maximum	0.2094	36.019	0.1565	0.2342	0.3387	0.1741
minimum	0.2066	35.997	0.1551	0.2326	0.3361	0.1731
range	0.0028	0.022	0.0014	0.0016	0.0026	0.0010
standard deviation (1 σ)	0.00144	0.0119	0.00070	0.00082	0.00145	0.00051
fluctuation coefficient	0.69	0.03	0.45	0.35	0.43	0.30
average (C)	20820	3601100	15580	23330	33780	17370
counting error (1 σ)	144.3	1898	124.8	152.7	183.8	131.8
1 σ /C (%)	0.69	0.05	0.80	0.65	0.54	0.76
average	0.2082	36.011	0.1558	0.2333	0.3378	0.1737
IBG (cal.)		0.1807		0.1919	0.1732	0.1619
difference		35.830		0.0414	0.1646	0.0118
correction coefficient		1		0.00116	0.00459	0.00033

Sample: high TiO ₂ -SiO ₂	TiK α position			BaL α position		
	BG1	peak	BG2	BG1	peak	BG2
1 (kcps)	0.2489	98.906	0.2127	0.3678	0.6841	0.2575
2	0.2504	98.877	0.2112	0.3605	0.6886	0.2546
3	0.2555	98.859	0.2095	0.3592	0.6842	0.2563
average	0.2516	98.881	0.2111	0.3615	0.6856	0.2561
maximum	0.2555	98.906	0.2127	0.2648	0.6886	0.2575
minimum	0.2489	98.859	0.2095	0.3592	0.6841	0.2546
range	0.0066	0.047	0.0032	0.0056	0.0045	0.0029
standard deviation (1 σ)	0.00346	0.0237	0.00160	0.00293	0.00257	0.00146
fluctuation coefficient	1.38	0.02	0.76	0.81	0.37	0.57
average (C)	25160	9888100	21110	36150	68560	25610
counting error (1 σ)	158.6	3145	145.3	190.1	261.8	160.0
1 σ /C (%)	0.63	0.03	0.69	0.53	0.38	0.62
average	0.2516	98.991	0.2111	0.3615	0.6856	0.2561
IBG (cal.)		0.2304		0.2390	0.2245	0.2158
difference		98.651		0.1225	0.4611	0.0403
correction coefficient		1		0.00124	0.00467	0.00041

Table 7 Overlap correction coefficients of the TiK α line overlap on the BaL α line

	BG1	Peak	BG2
low-Ti correction coefficients	0.00116	0.00459	0.00033
high-Ti correction coefficients	0.00124	0.00467	0.00041
average	0.0012	0.0046	0.0004

The BaL α intensity is calculated by multiplying 0.0046 to the net TiK α line intensity and subtracting the result from the net intensity of the BaL α line. The background position of the Ba is considered to be the

same as that of the TiK α line for the similar reason of the SC.

Table 8 Relationships between measurement positions and absorption edges

	RbBG1	YBG1	RbAE	Ypeak	YBG2	RbPeak	RbBG2
Wave length (pm)	79.95	80.64	81.55	83.08	85.45	92.56	100.84
2 θ	22.90	23.10	23.37	23.81	24.50	26.62	29.00
	SrBG1	ZrBG1	SrAE	Zrpeak	ZrBG2	Srpeak	SrBG2
Wave length (pm)	75.05	76.15	76.97	78.78	80.64	87.68	100.84
2 θ	21.48	21.80	22.04	22.56	23.10	25.15	29.00
	YBG1	YAE	NbBG1	Nbpeak	NbBG2	Ypeak	YBG2
Wave length (pm)	70.97	72.77	73.39	74.77	76.15	83.08	97.43
2 θ	20.30	20.82	21.00	21.40	21.80	23.81	28.00

AE: indicates absorption edge

Table 9 An example of the results corrected for the RbK β line overlap on the YK α line

Sample: Rb ₂ CO ₃ -SiO ₂	RbBG1	YBG1 *	YPeak	YBG2	Rbpeak	RbBG2
2 θ	22.90	23.10 *	23.81	24.50	26.62	29.00
1 (kcps)	3.5013	3.4862	59.105	3.7343	268.46	2.0768
2	3.5118	3.4802	59.105	3.7276	268.40	2.0690
3	3.5036	3.4864	59.072	3.7238	268.27	2.0782
average	3.5056	3.4843	59.094	3.7286	268.38	2.0747
maximum	3.5118	3.4864	59.105	3.7343	268.46	2.0782
minimum	3.5013	3.4802	59.072	3.7238	268.27	2.0690
range	0.0105	0.0062	0.033	0.0105	0.19	0.0092
standard deviation (1 σ)	0.00552	0.00352	0.0191	0.00532	0.097	0.00496
fluctuation coefficient	0.16	0.10	0.03	0.14	0.02	0.22
average (C)	350560	348430	5909400	372860	26838000	207470
counting error (1 σ)	592.1	590.3	2431.0	610.6	5181.0	455.5
1 σ /C (%)	0.17	0.17	0.04	0.16	0.02	0.22
* the relative position of the Rb absorption edge						
Sample: Blank-SiO ₂	RbBG1	YBG1 *	YPeak	YBG2	Rbpeak	RbBG2
2 θ	22.90	23.10 *	23.81	24.50	26.62	29.00
1 (kcps)	3.9737	3.8932	3.8442	3.2778	3.8694	2.0281
2	3.9800	3.8986	3.8480	3.2802	3.8575	2.0330
3	3.9812	3.8937	3.8519	3.2773	3.8642	2.0417
average	3.9783	3.8952	3.8480	3.2784	3.8637	2.0343
maximum	3.9812	3.8986	3.8519	3.2802	3.8694	2.0417
minimum	3.9737	3.8932	3.8442	3.2773	3.8575	2.0281
range	0.0075	0.0054	0.0077	0.0029	0.0119	0.0136
standard deviation (1 σ)	0.00403	0.00298	0.00385	0.00155	0.00597	0.00689
fluctuation coefficient	.10	0.08	0.10	0.05	0.15	0.34
average (C)	397830	389520	384800	327840	386370	203430
counting error (1 σ)	630.7	624.1	620.3	572.6	621.6	451.0
1 σ /C (%)	0.16	0.16	0.16	0.17	0.16	0.22

3.2 Determination of the Overlap Correction Coefficients of the RbK β Line to the YK α Line, the SrK β Line to the ZrK α Line, and the YK β Line to the NbK α Line

A blank SiO₂, Rb₂CO₃-SiO₂, SrCO₃-SiO₂, and Y₂O₃-SiO₂ mixtures were briquetted and subjected to qualitative analysis. Results showed that the back-

ground intensity changed discontinuously near the absorption edge; and, the background position to obtain the net intensity was different from the usual position because of high content of the coherent element. The latter problem can be avoided by locating a proper background position. The problem of background discontinuity is compensated for by

Table 10 Values used to estimate influences of contamination

	RbBG1	YBG1 *	YPeak	YBG2	Rbpeak	RbBG2
2θ	22.90	23.10 *	23.81	24.50	26.62	29.00
average (Si)	3.9783	3.8952	3.8480	3.2784	3.8637	2.0343
SiO ₂ value	—	3.9262	3.5955	3.3102	2.6027	—
BG (est.)	3.9783	3.8952	3.5610!	3.2784	2.5777!	2.0343

Average (Si) values shown are Rb contaminated values.
 X-ray intensities of Ypeak; (3.2784/3.3102)*3.5955
 X-ray intensities of Rbpeak; (3.2784/3.3102)*2.6027

Table 11 X-ray intensities of the blank-SiO₂ eliminated influences of contamination

	RbBG1	YBG1 *	YPeak	YBG2	Rbpeak	RbBG2
2θ	22.90	23.10 *	23.81	24.50	26.62	29.00
Average (RbSi)	3.5056	3.4843	59.094	3.7286	268.38	2.0747
BG (est.) (Si)	3.9783	3.8952	3.5610!	3.2784!	2.5777!	2.0343

Table 12 Overlap correction coefficients of the RbKβ line overlap on the YKα line

Sample: Blank-SiO ₂	RbBG1	YBG1 *	YPeak	YBG2	Rbpeak	RbBG2
2θ	22.90	23.10 *	23.81	24.50	26.62	29.00
BG (est.) (Si)	3.9783	3.8942	3.5610	3.274	2.5777	2.0343
Average (RbSi)	3.5056	3.4843	59.094	3.7286	268.38	2.0747
BG (cal.) RbSi)	(0.8812)	3.4324	3.6317	3.3435	2.6289	(1.0199)
difference	—	0.0519	55.462	0.3851	265.75	—
Correction coefficient		0.0002	0.2087	0.0014	1.0	

The values in the parentheses are correction coefficients to acquire background intensity. The value for RbBG1 is 3.5056/3.9783 and that for RbBG2 is 2.0747/2.0343

measuring the background of a blank SiO₂ standard. The background intensities used in this calculation should be measured at a higher position on the high energy side and a lower position on the low energy side than usual. The background positions at 23.10° for ZrBG2 and 21.80° for ZrBG1 and NbBG2 were selected for this experiment. Therefore, the former corrects the Rb and Sr overlap and the latter does the Sr and Y overlap. Table 8 summarizes the relationship between background positions, wave lengths used to determine absorption edges, and overlap correction coefficients.

The fine (1S) solar slit was selected for the low angle region of Nb to Pb because there were many peaks in close proximity to one another.

The determination of the overlap correction coefficient of the RbKβ line to the YKα line The X-ray intensities of the blank SiO₂ sample and the Rb₂CO₃-SiO₂ mixture were measured three times for 100 seconds. The results are listed in Table 9. The blank SiO₂ turned out to be contaminated with Rb during the briquette preparation. Therefore, the

background was estimated using the pure SiO₂ sample analyzed previously. (Later a blank SiO₂ was prepared again, and similar results were achieved.)

The Rb contamination influenced the Y peak (2θ angle: 23.81°) and Rb peak (2θ angle: 26.62). Table 9 shows the raw data. The X-ray intensities from the Rb contaminated blank SiO₂ were estimated using a different SiO₂ sample. Table 10 lists the values used for this correction and Table 11 shows the results.

The background shape was similar to that of the blank SiO₂. If one can assume that the discontinuous background intensity is due to the influence of the absorption edge, the background at the higher energy side of the absorption edge is given as follows:

$$I_{YBG1}\{\text{Blank-Si}\} * I_{RbBG1}\{\text{RbSi}\} / I_{RbBG1}\{\text{Blank-Si}\}$$

(It will be 3.8952*3.5056/3.9783 with real values.) The equation to calculate the background at the lower energy side is:

$$I_{YBG2}\{\text{Blank-Si}\} * I_{RbBG2}\{\text{RbSi}\} /$$

Table 13 An example of the results corrected for the SrK β line overlap on the ZrK α line

Sample: SrCO ₃ -SiO ₂	SrBG1	ZrBG1 *	ZrPeak	ZrBG2	Srpeak	SrBG2
2 θ	21.48	21.80 *	22.56	23.10	25.15	29.00
1 (kcps)	4.3210	4.2038	21.968	4.4364	276.33	2.0398
2	4.3100	4/2161	21.968	4.4403	276.26	2.0383
3	4.3220	4.2135	21.979	4.4338	276.20	2.0499
average	4.3177	4.2111	21.972	4/4368	276.26	2.0427
maximum	4.3220	4.2161	21.979	4.4403	276.33	2.0499
minimum	4.3100	4.2038	21.968	4.4338	276.20	2.0383
range	0.0120	0.0123	0.011	0.0065	0.13	0.0116
standard deviation (1 σ)	0.00666	0.00648	0.0064	0.00327	0.065	0.00631
fluctuation coefficient	0.15	0.15	0.03	0.07	0.02	0.31
average (C)	431770	421110	2197200	443680	27626000	204270
counting error (1 σ)	657.1	648.9	1482.0	666.1	5256.0	452.0
1 σ /C (%)	0.15	0.15	0.07	0.15	0.02	0.22
* the relative position of the Sr absorption edge						
Sample: Blank-SiO ₂	SrBG1	ZrBG1 *	ZrPeak	ZrBG2	Srpeak	SrBG2
2 θ	21.48	21.80 *	22.56	23.10	25.15	29.00
1 (kcps)	4.8603	4.6308	4.1326	3.8932	3.0632	2.0281
2	4.8643	4.6386	4.1484	3.8937	3.0632	2.0330
3	4.8761	4.6160	4.1339	3.8937	3.0590	2.0417
average	4.8669	4.6285	4.1383	3.8952	3.0618	2.0343
maximum	4.8761	4.6386	4.1484	3.8986	3.0632	2.0417
minimum	4.8603	4.6160	4.1326	3.8932	3.0590	2.0281
range	0.0158	0.0226	0.0158	0.0054	0.0042	0.0136
standard deviation (1 σ)	0.00821	0.01148	0.00877	0.00298	0.00242	0.00689
fluctuation coefficient	0.17	0.25	0.21	0.08	0.08	0.34
average (C)	486690	462850	413830	389520	306180	203430
counting error (1 σ)	697.6	680.3	643.3	624.1	553.3	451.0
1 σ /C (%)	0.14	0.15	0.16	0.16	0.18	0.22

Table 14 Overlap correction coefficients of the SrK β line overlap on the ZrK α line

Sample: Blank-SiO ₂	SrBG1	ZrBG1 *	ZrPeak	ZrBG2	Srpeak	SrBG2
2 θ	21.48	21.80 *	22.56	23.10	25.15	29.00
average (Si)	4.8669	4.2685	4.1383	3.8952	3.0618	2.0343
average (Sr-Si)	4.3177	4.2111	21.972	4.4368	276.26	2.0427
B _{gcal} (SrSi)	(0.8872)	4.1062	4.1554	3.9113	3.0744	(1.0041)
difference	—	0.1049	17.817	0.5255	273.19	—
correction coefficient		0.0004	0.0652	0.0019	1.0	

IRbBG2{Blank-Si}

The results are shown in Table 12. The reliability of this method can be confirmed by determining if the mass absorption coefficient of SiO₂ is constant at both the higher and lower sides of the absorption edge of an arbitrary element.

The overlap of the YK α line to the RbK β line was corrected by subtracting the net X-ray intensity of the RbK α line, 0.2087, 0.0002 and 0.0014, from Y_{peak}, YBGL and YBG2. However, the overlap of the SrK β line to the ZrBG2 must be corrected because the

measurement position of the YBGL was the same as that of the ZrBG2.

The determination of the overlap correction coefficient of the SrK β line to the ZrK α line The X-ray intensities of the Rb₂CO₃-SiO₂ mixture and the blank SiO₂ sample were measured three times for 100 seconds. The results are listed in Table 13 and the overlap correction coefficients are shown in Table 14.

The overlap influence of the SrK β line to the Zr peak, ZrBG1 and BrBG2 is 0.0652, 0.0004 and 0.0019 times respectively of the SrK α line. However, the overlap of the YKP line to the NbBG2 must be corrected because the measurement position of the

Table 15 An example of the results corrected for the YK β line overlap on the NbK α line

Sample: Y ₂ O ₃ -SiO ₂	YBG1 *	NbBG1	NbPeak	NbBG2	Ypeak	YBG2
2 θ	20.30 *	21.00	21.40	21.80	23.81	28.00
1 (kcps)	5.1169	13.391	11.570	5.5562	421.73	2.2336
2	5.0994	13.366	11.596	5.5683	421.50	2.2332
3	5.1094	13.360	11.578	5.5654	421.60	2.2357
average	5.1086	13.372	11.581	5.5633	421.61	2.2342
maximum	5.1169	13.391	11.596	5.5683	421.73	2.2357
minimum	5.0994	13.360	11.570	5.5562	421.50	2.2332
range	0.0175	0.031	0.026	0.0121	0.23	0.0025
standard deviation (1 σ)	0.00878	0.0164	0.0133	0.00632	0.115	0.00134
fluctuation coefficient	0.17	0.12	0.11	0.11	0.03	0.06
average (C)	510860	1336000	1158100	556330	42161000	223420
counting error (1 σ)	714.7	1156.0	1076.0	745.9	6493.0	472.7
1 σ /C (%)	0.14	0.09	0.09	0.13	0.02	0.21
Sample: Blank-SiO ₂	YBG1 *	NbBG1	NbPeak	NbBG2	Ypeak	YBG2
2 θ	20.30 *	21.00	21.40	21.80	23.81	28.00
1 (kcps)	6.1811	5.2554	4.9363	4.6308	3.8442	2.2158
2	6.1753	5.2579	4.9256	4.6386	3.8480	2.2127
3	6.1872	5.2700	4.9372	4.6160	3.8519	2.2201
average	6.1812	5.2611	4.9330	4.6285	3.8480	2.2162
maximum	6.1872	5.2700	4.9372	4.6386	3.8519	2.2201
minimum	6.1753	5.2554	4.9256	4.6160	3.8442	2.2127
range	0.0119	0.0146	0.0116	0.0226	0.0077	0.0074
standard deviation (1 σ)	0.00595	0.00781	0.00645	0.01148	0.00385	0.00372
fluctuation coefficient	0.10	0.15	0.13	0.25	0.10	0.17
average (C)	618120	526110	493300	462850	384800	221620
counting error (1 σ)	786.2	725.3	702.4	680.3	620.6	470.8
1 σ /C (%)	0.13	0.14	0.14	0.15	0.16	0.21

ZrG1 is the same as that of the NbBG2. The overlap correction at the YBGL and ZrBG2 positions (23.10°) is determined by subtracting

$$0.0002 * IRbK\alpha N_{peak} + 0.0019 * ISrK\alpha N_{peak}$$

from the background. Here, IRbK α N_{peak} and ISrK α N_{peak} are the net X-ray intensities.

The determination of the overlap correction coefficient of the YK β line to the NbK α line The X-ray intensities of the Y₂O₃-SiO₂ mixture and the blank SiO₂ sample were measured three times for 100

seconds. The results are listed in Table 15 and the overlap correction coefficients are shown in Table 16.

The overlap influence of the YK β line to the NbK α line is determined by subtracting 0.0158, 0.0193 and 0.0021 times the net YK α line from the Nb peak, NbBG1 and NbBG2 intensities, respectively. The net intensity of the YK α line must be corrected for the RbK α line overlap before the calculation. The overlap correction at the ZrBG1 and NbBG2 positions (21.80°) is calculated by the following equation:

$$0.0004 * ISrK\alpha N_{peak} + 0.0021 * IYK\alpha N_{peak}$$

Table 16 Overlap correction coefficients of the YK β line overlap on the NbK α line

	YBG1 *	NbBG1	NbPeak	NbBG2	Ypeak	YBG2
2 θ	20.30 *	21.00	21.40	21.80	23.81	28.00
average (Si)	6.1812	5.2611	4.9330	4.6285	3.8480!	2.2162
average (Y-Si)	5.1086	13.372	11.581	5.5633	421.61	2.2342
B _{gcal} (YSi)	(0.8265)	5.3038	4.9731	4.6661	3.5899	(1.0081)
difference	—	8.0682	6.6079	0.8972	418.02	—
correction coefficient		0.0193	0.0158	0.0021	1.0	
The X-ray intensity of blank-SiO ₂ at Ypeak position is the same as that of the RbK β line overlap on the YK α line because of the contamination.						

3.3 Summary of the Overlap Correction Coefficient

The overlap correction coefficient of the rika line to the $B\alpha$ BaLa line (2θ : 86.17°) is calculated by subtracting 0.0020 times the net TiK α line intensity from the X-ray intensity measured at $2\theta=87.18^\circ$.

$$I_{B\alpha peak} = I_{87.18} - 0.0020 * I_{TiK\alpha Npeak}$$

The overlap correction coefficient of the TiK α line to the BaL α line (with F-PC counter) The X-ray intensity of the BaL α line (2θ : 86.17°) is calculated by subtracting 0.0046 times the net TiK α line intensity from the X-ray intensity measured at $2\theta=87.18^\circ$.

$$I_{B\alpha peak} = I_{87.18} - 0.0046 * I_{TiK\alpha Npeak}$$

The overlap correction coefficient of the RbK β line to the YK α line The influence of the RbK β overlap to the YK α line intensity is eliminated by subtracting the 0.2087, 0.0002 and 0.0014 times the net intensity of the RbK α line (2θ : 26.62°) from the intensities at $2\theta=23.81^\circ$, 23.10° and 24.50° , respectively. At $2\theta=23.10^\circ$, the X-ray intensity is also corrected for the overlap of the SrK β line.

$$I_{Y\alpha peak} = I_{23.81} - 0.2087 * I_{RbK\alpha Npeak}$$

$$I_{BG24.5} = I_{24.5} - 0.0014 * I_{RbK\alpha Npeak}$$

$$I_{BG23.1} = I_{23.1} - (0.0002 * I_{RbK\alpha Npeak} + 0.0019 * I_{SrK\alpha Npeak})$$

The overlap correction coefficient of the SrK β line to the ZrK α line The influence of the SrK β line overlap to the ZrK α line intensity is eliminated by subtracting the 0.0652, 0.0004 and 0.0019 times the net X-ray intensity of the SrK α line (2θ : 25.25°) from the X-ray intensities at $2\theta=22.56^\circ$, 21.80° and 23.10° , respectively. At $2\theta=23.10^\circ$ and 21.80° , the X-ray intensities are also corrected for the overlap of the RbK β and YK β lines, respectively.

$$I_{Zr\alpha peak} = I_{22.56} - 0.0652 * I_{SrK\alpha Npeak}$$

$$I_{BG23.1} = I_{23.1} - (0.0019 * I_{SrK\alpha Npeak} + 0.0002 * I_{RbK\alpha Npeak})$$

$$I_{BG21.8} = I_{21.8} - (0.0004 * I_{SrK\alpha Npeak} + 0.0021 * I_{YK\alpha Npeak})$$

The overlap correction coefficient of the YK β line to the NbK α line The influence of the YK β line overlap to the NbK α line intensity is eliminated by

subtracting the 0.0158, 0.0193 and 0.0021 times the net X-ray intensity of the YK α line (2θ : 23.81°) from the X-ray intensities at $2\theta=21.40^\circ$, 21.00° and 21.80° , respectively. At $2\theta=23.10^\circ$, the X-ray intensity is also corrected for the overlap of the SrK β line.

$$I_{Nb\alpha peak} = I_{21.4} - 0.0158 * I_{YK\alpha Npeak}$$

$$I_{BG21.0} = I_{21.0} - 0.0193 * I_{YK\alpha Npeak}$$

$$I_{BG21.8} = I_{21.8} - (0.0021 * I_{YK\alpha Npeak} + 0.0004 * I_{SrK\alpha Npeak})$$

The overlap correction coefficients calculated above cannot be used with other experiments because they are condition and machine dependent.

4. Matrix Effect Correction Methods

X-ray intensities are affected not only by the concentration of analyzing elements, but also by coexisting elements. Influences from matrix effects must be eliminated in order to extract the X-ray intensity for the concentration of the elements of interest in quantitative analysis. In this chapter, methods to correct for matrix effects are discussed. The absorption effects of elements are summarized in Appendix 1.

1) The first method employs mass absorption coefficients. Norrish and Chappell (1967) showed that mass absorption coefficients can be obtained from calculation using chemical analysis and from direct measurements. Ikeda and Banno (1972) demonstrated that the results for Rb and Sr determined by both methods are comparable. The former was adopted for this experiment; the method has already been used for actual quantitative analysis (Banno and Chappell, 1969). Determination of mass absorption coefficients requires accurate chemical analysis (especially for major elements), as well as additional sample preparation for the actual measurement. The effect of the absorption correction utilizing this method can be confirmed by applying the absorption correction to the background X-ray intensity.

This method can correct for absorption but it cannot correct for enhancement or particle size effects on the X-ray intensity. Additionally, it does not analyze elements independently and it introduces errors from major elemental analysis to trace elemental analysis. Also, a sample whose major elements haven't been determined cannot be used as a standard.

2) A ratio method was used in this experiment. In this method, the net X-ray intensity is divided by the

background intensity and the quotient is used as the corrected X-ray intensity for a calibration curve (Peak over background method or INpeak/IBG method).

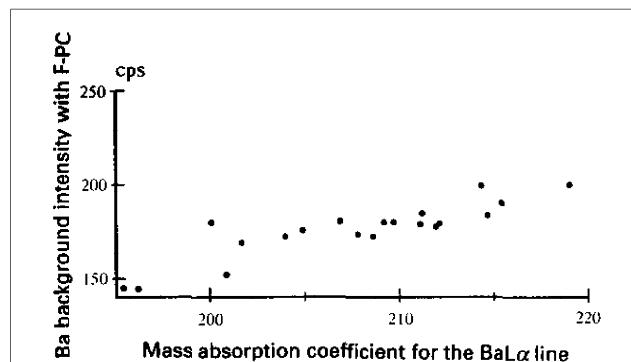


Fig. 1 Relationships between the background of Ba and the mass absorption coefficient of the BaL α line measured with an F-PC.

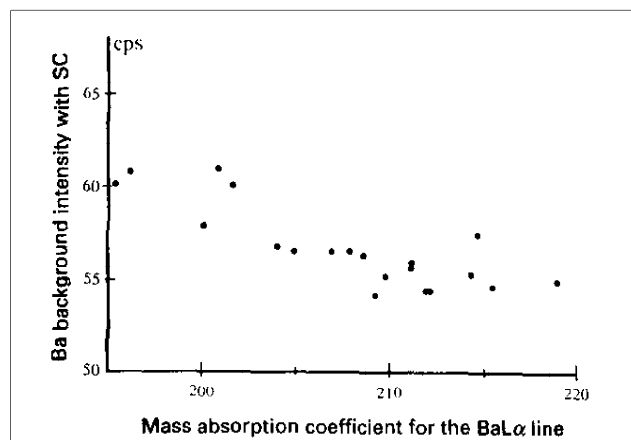


Fig. 2 Relationships between the background of Ba and the mass absorption coefficient of the BaL α line measured with an SC.

Champion et al. (1966) advocate this method. As it is known from the equations (1)-(3) in Appendix 1, the X-ray intensities of both peak and background are influenced from absorption and enhancement. Therefore, the ratio technique eliminates the matrix effects. Additionally, this method eliminates the influence from particle size. Consequently, the accuracy depends only on the counting error and the accuracy of standards. Samples that can be used as standards for the peak-to-background method are rock samples with concentrations of K, Rb and Sr that are determined using the highly accurate isotope dilution method.

This technique requires accurate measurement of the background and careful treatment of overlap to the background to minimize the analytical error.

(3) Finally, a newly developed method used in this work will be discussed. This correction method assumes that the background intensity would be the same if it were not for the matrix effect. The background intensity is then divided by the background of the specimen. It can be thought of as the reciprocal of the mass absorption coefficient of the specimen when that of the standard is normalized to 1. The net X-ray intensity divided by this quotient gives the corrected X-ray intensities. These results are used for a calibration curve. The advantages and disadvantages of this method are the same as those in (2).

The accuracy of analysis using a calibration curve corrected by any of the three methods is within the acceptable error.

Selection of F-PC or SC for Ba analysis Both F-PC and SC were utilized for Ba analysis because the counting rate is typically higher with the F-PC. However, for a series of measurements, the order of the corrected intensity (INPeak/IBG) by the SC

Table 17 Standards

	Method	
Rb,Sr	isotope dilution method	Ishizaka and Yanagi (1977) Ishizaka and Carlson (1983) Seki (1978)
Pb	carbon furnace atomic absorption method	Matumoto et al. (1986, 1988)
Th	nondestructive gamma-ray spectrometry	Komura et al. (1988)
K	isotope dilution method	Ishizaka and Yanagi (1977)
Na	flame photometry	Ishizaka and Yanagi (1977)
Cl	ion electrode	Yoneda et al. (1985)
Ba,Y	ICP	Uchida
Zr, Nb	mixture	Tatsumi and Gotoh
Ni	mixture+atomic absorption	atomic absorption method was done by Uchida

changes that by the FPC, in particular higher intensity samples. Moreover, the F-PC and SC give different Ba concentration at higher concentrations (F-PC always gives higher concentrations than SC).

The BaL α line overlap on the TiK α line was checked but no influence was found. Also, it was confirmed that the background of the BaL α line did not suffer any overlap influences. The relationship between the mass absorption coefficient of the BaL α line was then determined by calculations from the major element chemical analysis and the background X-ray intensities. The background intensity and mass absorption coefficient should satisfy equation (2) in Appendix 1. However, it is not F-PC (Fig. 1) but SC (Fig. 2) that satisfies the relationship. Therefore, the SC was selected for Ba measurements. The peak over background method corrects absorption, but when the absorption and mass absorption are not in inverse proportions, the correction does not necessarily work properly. The reason the F-PC does not satisfy the equation is unknown. However, it is certain that it influences all corrections. It may not satisfy equation (1) in Appendix 1, which is the basis of the quantitative analysis, or there may be some other causes that influence the X-ray intensities.

Consequently, it can be surmised that a clean calibration curve does not necessarily guarantee accurate quantitative analysis.

5. Selection of Standards

Table 17 lists standards. Some of them have previously been analyzed and their results have been published. Many standards were newly analyzed by Dr. T. Uchida at Nagoya Institute of Technology for this experiment. Generally, chemical analysis of natural rocks was utilized for standardization. Neither the standards provided by the Geological Survey of Japan nor the mixture of commercially available chemicals were used for the same reasons discussed in the quantitative analysis of major element in rock samples (Goto and Tatsumi, 1994). However, for Nb and Zr, we prepared standards using chemicals because no proper standards exist. SiO₂ was used as the matrix in these standards. Chemicals for Ni were also used and Dr. T. Uchida analyzed the mixture using atomic absorption because the actual purity of 99.9% NiO was only 95% pure.

Problems caused by the calibration curve using the mixture of chemicals and those caused by the curve based on X-ray intensities produced by the pure chemicals and compound may be different and

Table 18 Examples of relative errors

	Total concentration range	Concentrated	Medium	Dilute
Rb	—	1.99	1.72	9.51
Sr	2.31			
Pb	9.82			
Th	6.59			
Ba	5.07			
Y	2.35			
Zr	2.87			
Nb	1.44			
Ni	1.34*			
K	4.27			
Na+1	1.86			
Na+2	2.84			
Cl	7.16			

* result of regression analysis with a quadratic equation.
 +1 Ishizaka and Yanagi (1977)
 +2 wet chemical analysis by Dr. Haramura.

influence the results, although the effect has been neither checked nor confirmed.

Goto and Tatsumi prepared standards for Nb independently but identical calibration curves resulted.

6. Regression Calculation to Determine the Calibration Curve

The following points were addressed in the regression calculation.

- All values of standard were used for the calculation except when a value had an obvious problem.
- The regression calculation was done using a simple equation except when a quadratic equation had a clear advantage.
- In the Rb quantitative analysis, the regression analysis was done in three concentration ranges, high, medium and low, because of the presence of systematic errors.
- Standards used were provided by the Geological Survey of Japan for Pb and Th. However, values published in journals were used as shown in Table 17. JR-1 and JR-2 were excluded because when Dr. T. Uchida analyzed Ba and Y standards, the results were different from those of this study. Therefore, it was concluded that JR-2 is not homogeneous and varies bottle to bottle.

The calibration curve should not be extrapolated unless it is a linear regression equation and its

linearity is ensured by data. A calibration curve using a quadratic equation must never be extrapolated.

6.1 Counting Errors in X-ray Intensity

JB-1, JG-1a, JA-1 and JGb-1 were measured 10 times in order to estimate the intensity variation over ten days. The standard deviation of intensity (1σ) at each position was about twice as large as the counting error (1σ). The fluctuation may include many causes such as counting error, reproducibility of the machine and change of the surface condition of the sample. Influences on X-ray intensity (I_p/I_b) appear on the third digit after the decimal point or lower in the energy region higher than the $PbL\beta$ line. Therefore, when the corrected X-ray intensity was smaller than 0.01, it was not included in the regression analysis.

6.2 Relative Error in Quantitative Analysis

Table 18 summarizes the relative errors between chemical compositions determined by a calibration curve and by standards.

6.3 Examples of the Quantitative Analysis of Rocks Provided by Geological Survey of Japan

Results of quantitative analysis of rocks provided by the Geological Survey of Japan are summarized in Table 19. We did not extrapolate the calibration curve to complete this table. The standard deviations (1σ) are also listed for the samples measured repeatedly.

Major Elemental Analysis

7. The Purpose of Using Briquette Samples in Major Elemental Analysis

As was reported in the “Quantitative analysis of rock samples by an X-ray fluorescence spectrometer (1)”, it was found that pulverization induces various errors, although the errors are correctable. Briquette samples are free from those errors. Additionally, if the peak over background method used successfully in the trace element analysis is also effective in the major element analysis, one can use the same samples for both analyses. Therefore, briquette samples were used for the quantitative analysis of the major elements to investigate this possibility. Some satisfactory results were acquired for some elements. However, the accuracy for SiO_2 and Al_2O_3 turned out to be low; therefore, this method cannot be applied to all elements. SiO_2 is the most abundant in general rocks and Al_2O_3 is difficult to analyze even with wet chemical analysis. Details are discussed below.

8. Determination of Analysis Conditions

It was ensured that the dead time of the counter was corrected for and that full widths at half maximum (=FWHM) for high and low concentrations were similar. In quantitative analysis, the dead time becomes longer with high X-ray intensities. It reduces effective counting time and as a result, breaks the linear relation between concentration and X-ray intensity. The variation of peak width indicates that the peak shape changes at different concentrations. Either of them may result in non-linearity of the calibration curve. The linearity was checked by monitoring the X-ray intensities at 50 kV while changing the tube current from 2 to 50 mA (See Fig. Ap2-1). The peak width was confirmed from results of qualitative analysis done at low and high concentration.

8.1 Tube Current and Voltage

The scintillation counter (SC) and the proportional counter (PC) should be used below 1000 kcps and 2000 kcps respectively to avoid saturation. Counters become saturated when the X-ray intensity is strong. Therefore, one should consider the possibility of saturation with elements at high concentrations or with small mass absorption coefficients. The $SiK\alpha$ line and $MgK\alpha$ line (especially from peridotite) are expected to have large counts. The $FeK\alpha$ line is also strong because of its small absorption coefficient. If pure material is available, it is desirable to add it to standards. In this experiment, Al_2O_3 was added and the $AlK\alpha$ line was studied; the highest grade SiO_2 and Al_2O_3 were used. MgO was taken from the JP-1 (MgO : 44.72 wt%) standard provided by the Geological Survey of Japan. Amphibolite (Fe_2O_3 : 17.01 wt%) was employed for Fe_2O_3 . The results shown in Table 20 indicate that the same voltage and current (50 kV, 50 mA) could be used for these elements.

Although it was not necessary to control X-ray intensity in this experiment, the following methods can be used to reduce intensity without changing the tube voltage and current.

- Switching the solar slit from coarse (3S) to fine (1S).
- Insertion of an absorber. (A 3370 spectrometer has only one absorber that reduces intensity to 1/10).
- Reduction of the activation area. There are two methods: changing the mask of the sample holder or modifying the parameter of the measurement. The

Table 19 An example of analysis of rock standard provided by the Geological Survey of Japan

	JB-1	JG-1a	JA-1	JGb-1	JB-1a	JB-2	JB-3	JA-2	JA-3		
Rb	41.7	175	11.7	5.4	40.5	6.1	15.0	76.2	38.1		
	0.2	0.8	0.2	0.1							
Sr		188	262	310		170		250	287		
		0.7	1.4	1.3							
Pb	6.8	27.8	6.3		6.0	5.4	4.8	21.5	8.5		
	0.4	0.3	0.4								
Th	9.6	12.4			9.8			4.8	2.9		
	0.5	0.4									
Ba	477	426	279	49.5		202	233	285	297		
	7.3	12.3	7.5	7.8							
Y	21.1		27.4	8.6	21.2	21.1	23.3	16.4	19.2		
	0.2		0.3	0.2							
Zr	133	105	82.2	26.1	135	44.2	90.3	112	116		
	1.2	1.0	0.9	0.5							
Nb	29.4	9.4			23.5			8.0			
	0.2	0.1									
Ni	105				104			120			
	0.7										
	JG-2	JG-3	JR-1	JR-2	JLK-1	JSL-1	JSD-1	JF-1	JF-2	JDO-1	JLS-1
Rb	297	73.3	254	201	158	125	72.9	257	210		
Sr			28.2		70.9	195	349	167	194	110	252
Pb	32.1	12.0	19.1	21.6		19.9	14.2				
Th	33.2	8.0	31.2		22.1	11.1	3.9				
Ba	272	112	83.4	73.4		310			271		285
Y		16.2					13.8			10.5	
Zr	94.5	145	97.1	92.6	138	172	124		32.9		
Nb	12.2	5.1	13.0	15.5	13.5	8.4	10.0				

Table 20 Examples of counting rates for concentrated samples

	Counter	Counting rates (kcps)
SiO ₂ (pure chemical)	F-PC	498.55
Al ₂ O ₃ (pure chemical)	F-PC	221.81
MgO (JP-1; Horoman peridotite)	F-PC	81.792
Fe ₂ O ₃ (hornblende)	SC	417.84

former influences all elements and the latter influences desired elements.

d) Using a different diffraction crystal. Every method above also reduces background intensities; therefore, the background should be measured longer to improve the counting statistics.

8.2 Determination of Peak and Background Positions, Solar Slits, Upper and Lower Limits of the Peak Height Analyzer, and Counting Time

These conditions should be determined through qualitative analysis so that the peak can be isolated and the background positions can be readily and clearly determined. The peak positions are determined using pure material or a sample that has the desired

element at a high concentration. The background intensity near a strong peak tends to be higher; therefore, the background positions should be free from the peak X-ray intensity and any interference.

The background should be measured at both high and low angle sides, but it is measurable only on one side with some elements. There is a method to estimate the background at a peak position from the slope acquired from qualitative analysis of SiO₂ or Al₂O₃; however, this method was not investigated for this work. Neighboring peaks that overlap can be separated using the fine (1S) solar slit.

The upper and lower limit of the pulse height analyzer (PHA) should be adjusted when the

influence from high-order radiation is significant. The window of the PHA was narrowed down to 150-250 from 100-300 for the MgK α and NaK α lines because the third order X-ray of the CaK α line overlaps with the MgK α line; and, the highorder X-ray radiation from Ti in the diffraction crystal (TAP) effects the NaK α line. It was found that the TiK β , VK β and CrK β lines overlap the VK α , CrK α and MnK α lines, respectively. When MnO is analyzed, every overlap should be checked and corrected if necessary. The counting time for the background was selected for the best counting statistics. Table 21 summarizes the values.

The background of the SiK α line is measured only at the higher angle side because of the K α and K β line overlap the background at the low angle side and increase the X-ray intensity.

The X-ray intensities at the high angle side of the AlK α and KK α lines are not at the background level even at 147°, the mechanical angle limit.

The backgrounds at the high angle side of the MgK α and NaK α lines were set equal. The AlK α and MgK β lines overlap the background at the low angle side of the MgK α line and the NaK α and MgK α lines influence the background at the high angle side.

At the low angle side of the NaK α line, the MgK α line affects the background intensity; therefore, the background can be measured only at the low angle side, especially for peridotite analysis.

The background of the high angle side of the CaK α line suffers overlap of the KK β line and CaK α line itself.

9. Comparison of Standards by the Glass Bead Disk Method, the Peak Over Background Method, and the Semifundamental Parameters Method

The feasibility of using briquette samples for quantitative analysis was examined because this method is free from errors that are introduced in the preparation of glass beads such as weighing, distortion and crystallization of the bottom of the alloy tray and conditions of the bead sampler. Also, it was expected that briquette samples would produce results as accurate as glass beads when the peak over background method and semifundamental parameters methods were applied. The peak over background method gave satisfactory results in the trace element analysis and the semifundamental parameters method worked well in quantitative analysis when the number of standards was limited. The peak over background and semifundamental parameters methods produced results as precise as the glass bead method in the trace element analysis of K₂O and Na₂O. However, the results of SiO₂ and Al₂O₃ analysis were far from the values determined by wet analysis. The inaccuracy of the analysis of these elements reduces the merit of using briquette samples in the quantitative analysis of major elements. However, the briquette method may be a good choice for the analysis of a major element when it is at relatively low content and unusually precise standards for the element are available.

10. Why Quantitative Analysis Cannot Be Done by the Briquette Method

The results of analysis change due to the composition and condition of the matrix. The effect of

Table 21 Measurement conditions employed for the Rigaku 3370 spectrometer

Voltage: 50 kV Tube current: 50 mA

Anode: Rh (Rhodium) (X-ray tube: Rhodium tube)

Beam path: vacuum

Element (X-ray lines)	Peak	BG1 (low)	BG2 (high)	Diffraction crystal	Slit	Counter	Time Peak/BG	PHA
SiK α	109.14		120.00	PET	coarse	F-PC	20s/100s	100-300
TiK α	86.20	82.50	89.50	LiF	coarse	SC	100s/100s	100-300
AlK α	114.82	137.00		PET	fine	F-PC	20s/100s	100-300
FeK α	57.575	55.00	65.00	LiF	fine	SC	50s/100s	100-300
FeK α	57.575	55.00	65.00	LiF	coarse	SC	50s/100s	100-300
MgK α	45.26		59.00	TAP	coarse	F-PC	50s/100s	150-250
CaK α	113.125	108.00		LiF	coarse	F-PC	50s/100s	100-300
NaK α	55.20		59.00	TAP	coarse	F-PC	100s/100s	150-250
KK α	136.64	128.20		LiF	coarse	F-PC	100s/100s	100-300
PK α	141.00		145.00	Ge	coarse	F-PC	100s/100s	100-300

the composition of the matrix, which is summarized in Appendix 1, is related to X-ray absorption and the excitation by X-rays. The influence from the condition of the matrix rises from the difference in phases, that is the fluctuation of the X-ray intensity caused by the variation in bonding status. Dilution reduces the matrix effect and vitrification minimizes chemical difference in the glass bead analysis. This can be confirmed by agreement between calculated and measured mass absorption coefficients and the deviation from the calibration curve. The peak over background method applied to the briquette samples can eliminate the matrix effect (X-ray absorption and excitation) and the particle size effect of minerals, but the effect resulting from the matrix status may remain. This effect may be significant when the grain is formed with various minerals or consists of glass. In X-ray fluorescence analysis, the surface of samples is assumed to be homogeneous. However, this condition may not be achieved at longer wavelengths. When the mineral grain contains glass fragments, homogeneity of samples cannot be achieved. Heterogeneity of the X-ray source has significant effects on quantitative analysis. However, this does not mean that briquette samples are always inappropriate for quantitative analysis. If the fluctuation of the X-ray intensity caused by the heterogeneity of the surface of the sample is smaller than the error of wet chemical analysis, the effect is insignificant and quantitative

analysis can be done and vice versa. For example, the error of wet chemical analysis of major element is 0.2-0.3wt%. This suggests that the relative error should be smaller than 0.5% to analyze a rock sample containing 50% of SiO₂. When the X-ray intensity from fluctuation of the heterogeneity of surface is

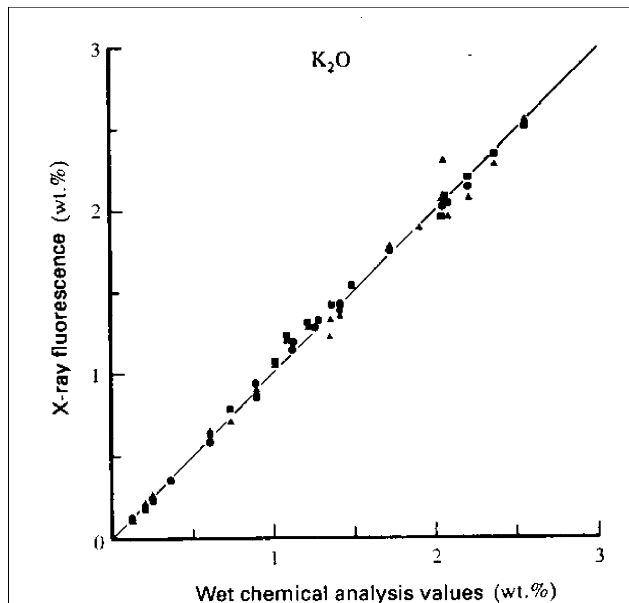


Fig. 3 Wet chemical analysis of the standard K₂O and the results of quantitative analyses for three methods: glass bead method (●), peak over background method (△) and semifundamental parameter method (■).

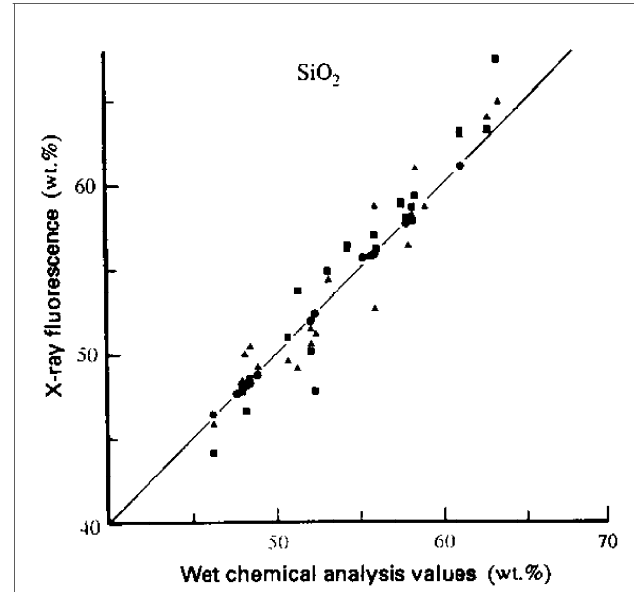


Fig. 4 Wet chemical analysis of the standard SiO₂ and the results of quantitative analyses for three methods: glass bead method (●), peak over background method (△) and semifundamental parameter method (■).

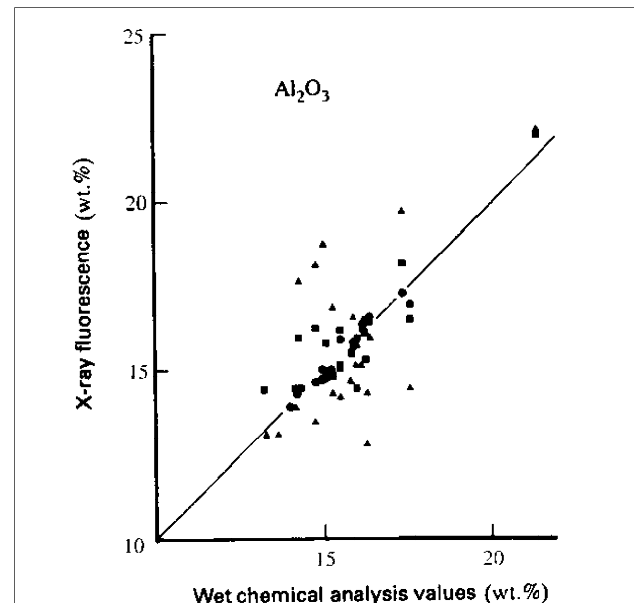


Fig. 5 Wet chemical analysis of the standard Al₂O₃ and the results of quantitative analyses for three methods: glass bead method (●), peak over background method (△) and semifundamental parameter method (■).

larger, quantitative analysis will not be successful. The counting error must be kept at lower level to achieve the accuracy applying the peak over background method. Major elemental analysis uses the long wavelength and low energy X-ray region where absorption becomes maximum. Absorption significantly reduces the background level; longer counting time is needed to compensate for absorption.

The main components of major elements are the light elements that have special lines in the low energy region. The radiation from light elements is weak. The matrix effect and the heterogeneity of the surface can amplify the intensity fluctuation. The radiation from heavy elements is stronger, therefore would give more accurate results.

11. Summary

The first half of this paper summarizes the techniques to perform accurate quantitative analysis of trace elements. The overlap effect, the matrix effect and the selection of standards are discussed in detail.

The second half investigates the limitations using briquette samples for quantitative analysis. It is apparent that the desired accuracy cannot be achieved for all elements and the conclusion is discouraging. However, it was found that results are as accurate as those from the glass bead method and using briquette samples is applicable to some elements.

Briquettes might be a better choice over glass beads for major elements at low concentrations when well-established standards are available. Despite that, when K_2O and Na_2O were examined applying methods for trace element analysis in this experiment, satisfactory results were achieved.

Results indicate the possibility of some misunderstanding due to theoretical or practical considerations of X-rays. We invite comments, particularly on the disagreement between calculated and real values for Ba measured with SC and F-PC detectors.

Acknowledgment

We would like to express our thanks to many individuals. The editor of *The Rigaku Journal* allowed us to publish this report, which is more like a lab manual than a paper. People of Rigaku Industrial Corp., especially at the Analytical Laboratory who made arrangements for our convenience. Dr. Tetsuo Uchida at Nagoya Institute of Technology analyzed Ba and Y with ICP, Ni with atomic absorption to establish standards. Prof. Kyoichi Ishizaka at Kyoto University and Dr. Tatsuya Seki at Okayama

University of Science allowed us to use their precious specimen as standards. Dr. Takeshi Mori at Kyoto University read the entire first manuscript and provided very important advice. Prof. Shohei Banno at Kyoto University provided consultation on many occasions. Also, there are many people who contributed to our experiment and manuscript, although we cannot name all of them. Thanks are due to all of the above individuals.

Appendix 1. Influences from the Composition of Major Elements on X-ray Intensities

Influences from the composition of the elements in rocks on X-ray intensities can be treated quantitatively by calculation of mass absorption coefficients when interference of noise is eliminated. The mass absorption coefficient and the influence of excitation energy are constant for an arbitrary wave length (that is, at a certain energy level). Norrish and Chappell calculated mass absorption coefficient $(\mu/\rho)\lambda$, net X-ray peak intensity (I_p) and composition (C) using the following equation (1967).

$$(\mu/\rho)\lambda * I_p / C = \text{constant}(K_p) \quad (1)$$

Mass absorption coefficients were calculated from the results of major elemental analysis and mass absorption coefficients listed in Table 3 in the article, "X-ray micro-analyzer", by Uchiyama. Table Apl-1 summarizes the results. Influences on trace elemental analysis from glass bead sample preparation, which is usually employed for major elemental analysis, were also shown for 1:5 and 1:10 mixtures of sample and lithium borate anhydride. The shift of the mass absorption coefficient for the 1:10 mixture is still large; therefore, the influence of chemical composition is significant.

If the net X-ray intensity and mass absorption coefficient satisfy equation (1), the background intensity (I_b) should satisfy the similar equation:

$$(\mu/\rho)\lambda * I_b = \text{constant}(K_b) \quad (2)$$

This equation means that the mass absorption coefficient is proportional to the background X-ray intensity. Fig. Apl-1 shows an example, the relation between the mass absorption coefficient and background of Rb. In trace elemental analysis, Ba measured with an F-PC is the only exception for this relationship as is shown in Fig. 1.

The discussion above implies that the mass absorption coefficient has significant influence on quantitative analysis of trace elements. Equations (1)

and (2) indicate that elimination of the absorption effect is the most critical correction in quantitative analysis by X-ray fluorescence.

The absorption can be corrected for properly by using the calculated mass absorption coefficients when the composition of major elements is well determined. Norrish and Chappell et al. (1967) summarize this method.

Equation (1) divided by (2) gives,

$$I_p/I_b = kC \quad (3)$$

Here, k is K_p/K_b , a constant. Equation (3) indicates that I_p/I_b is proportional to the content (C). Mass absorption coefficients can be eliminated this way.

The effect of excitation is discussed herein. The extent of the intensity fluctuation caused by the X-ray excitation is the result of the multiplication between intensity and the excitation itself. This means that coefficients corresponding to the mass absorption coefficients in equations (1) and (2) can be assumed for excitation for both net peak and background intensities. Therefore, the net peak intensity to background ratio given by (3) excludes influences from excitation as well as from absorption. The influences from particle size can be eliminated similarly.

Appendix 2. Preparation of Mixture

2.1 Standards

Standards did not give accurate values for Nb and Zr in this experiment. Therefore, other standards were prepared mixing pure chemicals.

The preparation of standards for Nb and Zr is summarized below as an example. The matrix for all

standards is SiO₂, which was ground with an automatic agate mortar for over two hours, baked at 950°C for three hours and cooled in a desiccator.

The chemicals used for Nb and Zr standards were niobium pentoxide (Nb₂O₅, Wako Chemicals Co., 99.9% purity) and zirconium dioxide (ZrO₂, Mitsuwa Chemicals Co., 99.9% purity). These two chemicals were dried at 110°C for 24 hours before preparation. Impurities were checked with 0.1 g of Nb₂O₅ and ZrO₂ in 10 g SiO₂ and trace amounts of Hf from ZrO₂ were detected. Therefore, only Nb₂O₅ will be explained.

SiO₂ and some acetone from Wako Chemicals Co. were put in an agate mortar, washed with acetone, and ground for over 30 minutes. The resulting powder was gathered and stored carefully. The agate mortar

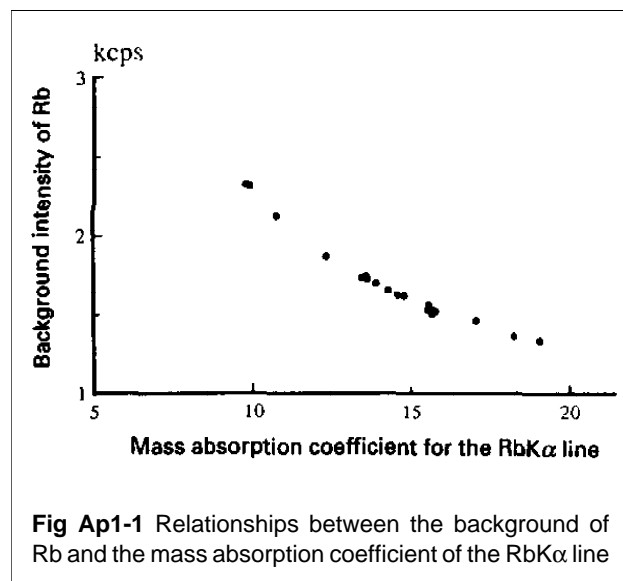
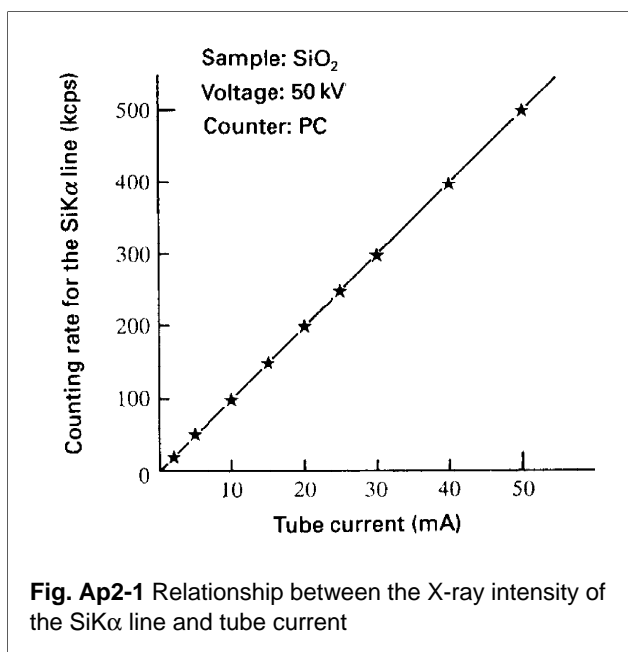


Fig Ap1-1 Relationships between the background of Rb and the mass absorption coefficient of the RbKα line

Table Ap1-1 Ranges of the mass absorption coefficients acquired from rocks having various chemical compositions.

	NbKα	ZrKα	Y-Kα	SrKα	RbKα	PbLα	BaLα	NiKα	S-Kα	ClKα
minimum	5.3	6.1	7.1	8.3	9.7	18.6	185.2	48.5	871.3	611.2
maximum	12.9	14.9	17.2	20.0	23.4	44.7	310.1	115.0	1093.7	766.5
dissolvent	1.21	1.37	1.46	1.86	2.21	4.30	48.5	11.31		
mixing ratio 1:5 (sample: dissolvent)										
	NbKα	ZrKα	Y-Kα	SrKα	RbKα	PbLα	BaLα	NiKα		
minimum	1.89	2.16	2.40	2/93	3.46	6.68	71.3	17.5		
maximum	3.16	3.63	4.08	4.88	5.74	11.03	92.1	28.6		
Mixing ratio 1:10 (sample: dissolvent)										
	NbKα	ZrKα	Y-Kα	SrKα	RbKα	PbLα	BaLα	NiKα		
minimum	1.58	1.80	1.97	2.45	2.89	5.60	60.9	14.7		
maximum	2.27	2.60	2.89	3.51	4.14	7.97	72.3	20.7		



was washed with acetone and used in the following procedures.

First, a stock mixture containing 0.5g of Nb₂O₅ in 10 g of SiO₂ was prepared and diluted later with SiO₂ to make standards at specific concentrations.

A Mettler digital balance that can measure 5 digits below the decimal point was used. The balance was leveled and checked for any object which may interfere with weighing; then, the zero point was adjusted. When a balance has dials to switch weights, they should always be turned in the same direction from low to high. For example, when one needs to change the weight one digit above, one should first turn the fine adjustment down to and past zero, then turn it back up to zero. (See the manual for more details.)

One-half gram (0.5g) of Nb₂O₅ was measured with the balance. Aluminum foil cleaned with acetone was used rather than weighing paper. Then, the weighed chemical was transferred to the agate mortar without any loss. The aluminum foil was washed with acetone down to the mortar. (This is why aluminum foil instead of a weighing paper is used.) Then equivalent amounts of SiO₂ (less than three times) were measured and added to the mortar. The remaining SiO₂ was again washed with some acetone into the mortar. (Note: If any chemical is spilled, one has to restart from weighing again. If too much acetone is added, it should be evaporated until it reduces to an appropriate volume. The mortar and pestle should be covered with aluminum foil cleaned with acetone

during the evaporation. One should continue to mix the sample even when the volume of acetone decreases. The mixing and grinding effects reach maximum with very little acetone.) The mixing was continued for 10 minutes after the acetone evaporated completely. The sample sticking to the mortar and pestle was scraped off with a piece of film wiped with acetone. (The film should be made of material insoluble to acetone such as polypropylene.) The sample was mixed for another 10 minutes. The amount of sample in the mortar was 2 g at the most at this stage. Some SiO₂, less than three times of the ground sample, was added and the mixing procedure above was repeated. When it was done, the sample was gathered and transferred to a clean glass bottle with a label. The sample was dried in a desiccator to remove moisture. This was diluted to prepare standards at various concentrations.

2.2 Standards for the Overlap Correction

The procedure above applied to the preparation of standards for the overlap correction. 10 g of SiO₂ ground with an automatic grinder and dried at 1100C was used for the preparation of standards. 0.1 g of Nb₂O₅, ZrO₂, Y₂O₃, SrCO₃, Rb₂CO₃ and BaCO₃ were weighed and mixed. Two standards, high and low content, were prepared for TiO₂ and used for the overlap correction. The low and high content standards had 0.2 g and 0.5 g of TiO₂, respectively. Dilution was necessary because excess counting results in longer dead time and therefore results in large errors. SC and F-PC must be used below 1000 and 2000 kcps, respectively. The counter was corrected for dead time and the output values were already corrected. This correction was confirmed by a SiO₂ briquette sample measured at a constant voltage for the SiKα (50 kV) and with variable tube current. It was found that it had high linearity from 2 mA to 50 mA (Fig. Ap2-1).

References

- Banno, S. and Chappell, B. W. (1969). X-ray fluorescent analysis of Rb, Sr, Y, Pb and Th in Japanese Paleozoic slates. *Geochemical Journal* **3**, 127-134.
- Champion, K. P., Taylor, J. C. and Whittem, R. N. (1966). Rapid X-ray fluorescence determination of traces of strontium in samples of biological and geological origin. *Analytical Chemistry* **38**, 109-122.
- Goto, A. and Tatsumi, Y. (1994). Quantitative analysis of rock samples by an X-ray fluorescence spectrometer (1). *The Rigaku Journal* **11**, 40-59.
- Ikeda, Y. and Banno, S. (1972). The method of Rb and Sr analysis in some standard rocks by X-ray fluorescence. *Journal of Japanese Association of Mineralogists*,

- Petrologists and Economic Geologists **67**, 262-266 (in Japanese with English abstract).
- Ishizaka, K. and Yanagi, T. (1977). K, Rb and Sr abundances and Sr isotopic composition of the Tanzawa granitic and associated gabbroic rocks, Japan: low potash island arc plutonic complex. *Earth and Planetary Science Letters* **33**, 345-352.
- Ishizaka, K. and Carlson, R.W. (1983). Nd-Sr systematics of the Setouchi volcanic rocks, southwest Japan: a clue to the origin of orogenic andesite. *Earth and Planetary Science Letters* **64**, 327-340.
- Komura., K., Tan, K. L. and Ueno, K. (1988). Uranium, thorium and potassium contents in eighteen geochemical reference samples issued from the Geological Survey of Japan. *Geostandards Newsletter* **12**, 371-374.
- Matsumoto, A., Hirao, Y., Iwasaki, M. Fukuda, E., Hanami, H., Nara, S. and Kimura, K. (1986). Determination of lead in environmental samples by graphite furnace AAS. *Analytical Chemistry (Bunseki Kagaku)* **35**, 590-597 (in Japanese with English abstract).
- Matsumoto, A., Saito, Y., Hirao, Y. and Kimura, K. (1987). Determination of lead in standard rocks by graphite furnace AAS. *Analytical Chemistry (Bunseki Kagaku)* **37**, 112-115 (in Japanese with English abstract).
- Norrish, K. and Chappell, B. W. (1967). X-ray fluorescence spectrography. In J. Zussman ed. 'Physical methods in determinative mineralogy', Academy Press London, 161-214.
- Seki, T. (1978). Rb-Sr geochronology and petrogenesis of the late Mesozoic igneous rocks in the inner zone of the southwestern part of Japan. *Memoirs of the Faculty of Science, Kyoto University, Series of Geology and Mineralogy* **45**, 71-110.
- Uchiyama, I., Watanabe, A. and Kimoto, S. (1972). X-ray microanalyser. *Nikkan Kohgyou Press*, pp 243. (in Japanese).
- Yoneda, S., Haramura, H., Urabe, T. and Matsumoto, R. (1985). Determination of chlorine content in volcanic rocks by X-ray fluorescence analysis. *Journal of Japanese Association of Mineralogists, Petrologists and Economic Geologists* **80**, 363-368 (in Japanese with English abstract).